Synthesis and Photovoltaic Properties of 2,6-Bis(2-Thienyl) Benzobisazole and 4,8-Bis(thienyl)-Benzo[1,2-*B*:4,5-*B*′]Dithiophene Copolymers

Achala Bhuwalka,[1] Monique D. Ewan,[1] Moneim Elshobaki,[2,3] Jared F. Mike,[1] Brian Tlach,[1] Sumit Chaudhary,[4] Malika Jeffries-EL[1]

[1]Department of Chemistry, Iowa State University, Ames, Iowa 50011
[2]Department of Materials Science and Engineering, Iowa State University, Ames, Iowa 50011
[3]Department of Physics, Mansoura University, Mansoura 35516, Egypt
[4]Department of Electrical and Computer Engineering, Iowa State University, Ames, Iowa 50011
Correspondence to: M. Jeffries-EL (E-mail: malikaj@iastate.edu)

Received 5 June 2015; accepted 16 July 2015; published online 00 Month 2015
DOI: 10.1002/pola.27793

ABSTRACT: In an effort to design efficient low-cost polymers for use in organic photovoltaic cells the easily prepared donor–acceptor–donor triad of a either *cis*-benzobisoxazole, *trans*-benzobisoxazole or *trans*-benzobisthiazole flanked by two thiophene rings was combined with the electron-rich 4,8-bis(5-(2-ethylhexyl)-thien-2-yl)-benzo[1,2-*b*:4,5-*b*′]dithiophene. The electrochemical, optical, morphological, charge transport, and photovoltaic properties of the resulting terpolymers were investigated. Although the polymers differed in the arrangement and/or nature of the chalcogens, they all had similar highest occupied molecular orbital energy levels (−5.2 to −5.3 eV) and optical band gaps (2.1–2.2 eV). However, the lowest unoccupied molecular orbital energy levels ranged from −3.1 to −3.5 eV. When the polymers were used as electron donors in bulk heterojunction photovoltaic devices with $PC_{71}BM$ ([6,6]-phenyl C_{71}-butyric acid methyl ester) as the acceptor, the *trans*-benzobisoxazole polymer had the best performance with a power conversion efficiency of 2.8%. © 2015 Wiley Periodicals, Inc. J. Polym. Sci., Part A: Polym. Chem. **2015**, *00*, 000–000

KEYWORDS: conjugated polymers; heteroatom containing polymer; photovoltaic cells; synthesis

INTRODUCTION Organic photovoltaic cells (OPVs) continue to garner a large amount of interest due to their potential for use in the development of lightweight and large area panels for efficient solar energy conversion. Currently, the most efficient OPVs are based on the bulk-heterojunction concept in which an electron-accepting material, such as a functionalized fullerene, is blended with an electron-donating conjugated polymer.[1] Achieving high power conversion efficiency (PCE) in these systems requires concurrent optimization of several parameters including the nanoscale morphology of the polymer film formed upon blending with the donor-conjugated polymers, the fullerene acceptor, and the alignment of energy levels of these two components.[2] In an effort to optimize the properties of the donor polymers, there has been extensive research on the design and synthesis of new materials. A popular approach is the synthesis of polymers composed of alternating electron-rich and electron-poor moieties as the intramolecular charge transfer between these groups can be modified by adjusting the strength of the two monomers, thereby enabling tuning of the polymer's highest occupied molecular orbital (HOMO) and lowest unoccupied molecular orbital (LUMO) levels.[3] Although there are many known donor–acceptor conjugated polymers, only a few combinations have resulted in high PCEs. Moreover, many of these polymers utilize complex heterocycles that are challenging to synthesize and purify on large scale.[2,4]

Accordingly, benzo[1,2-*d*;5,4-*d*′]bisoxazole (*cis*-BBO), benzo-[1,2-*d*;4,5-*d*′]bisoxazole (*trans*-BBO), and benzo[1,2-*d*;4,5-*d*′]bisthiazole (*trans*-BBZT) are particularly promising for the development low-cost solution processible OPVs. Collectively referred to as the benzobisazoles, these electron-deficient heterocycles are present in a variety of materials including high-performance rigid-rod polymers,[5] nonlinear optical materials,[6] emissive polymers for use in organic light-emitting diodes,[7] electron-transporting layers,[8] field-effect transistors (OFET)s,[9] and OPVs.[9(c),10] Benzobisazoles have planar conjugated structure that facilitates $\pi-\pi$ stacking, improving charge carrier mobility.[8,9(d)] Additionally, polybenzobisazoles are among some of the most thermally and environmentally stable materials known, which is beneficial for long-term device stability.[5] As a result of their origins as high-performance materials, the monomers required for the

Additional Supporting Information may be found in the online version of this article.

synthesis of benzobisazoles can be prepared in large quantities, and purified without the use of column chromatography, making scale-up feasible.[5(a,b),11] Historically, the use of polybenzobisazoles was hampered by their poor solubility and the harsh conditions used for their synthesis. However, new synthetic methods have enabled the development of solution processable polybenzobisazoles.[7(f),9(c),10(a)]

Previously, we reported the synthesis and photovoltaic properties of copolymers comprising a donor–acceptor–donor tri triad of a benzobisazole flanked by two thiophene rings and 3,3′-dioctylbithiophene.[10(c)] These copolymers exhibited hole mobilities as high as 4.9×10^{-3} $cm^2V^{-1}s^{-1}$ when used in OFETs and modest PCEs up to 1.14%, with the *trans*-BBO polymer giving the best performance in both devices. In an effort to improve upon the performance of these polymers, we replaced the bithiophenes with benzo[1,2-*b*:4,5-*b*′]dithiophene (BDT). This electron-rich building block has a planar structure that facilitates $\pi-\pi$ stacking thus improving hole mobility.[12] As a result, there are several copolymers comprised of BDT and various electron-deficient moieties with reported PCEs approaching the 10% PCE sought after for commercial viability.[13] In this work, we have utilized the two-dimensional donor moiety 4,8-bis(5-(2-ethylhexyl)thien-2-yl)-benzo[1,2-*b*:4,5-*b*′]dithiophene. Replacing the electron-rich alkoxy-side chains with thiophene rings lowers the HOMO level of the resulting polymers, while the extended conjugation created by the flanking thiophene rings increases absorption. As a result, polymers made from thiophene-substituted BDTs often have better OPV performance than their alkoxy-substituted analogs.[14] This selection proved to be advantageous as when the polymers were used as electron donors in bulk heterojunction photovoltaic devices with $PC_{71}BM$ as the acceptor, the *trans*-benzobisoxazole polymer had the best performance with a PCE of 2.8%. This nearly a threefold increase over the previously reported devices based on the bithiophene comonomers,[10(c)] and rivals the performance of our copolymers with dithienylsilole.[15]

EXPERIMENTAL

Materials and General Experimental Details

Toluene was dried using an Innovative Technologies solvent purification system. All other chemical reagents were purchased from commercial sources and used without further purification unless otherwise noted. 4,8-bis(5(2-ethylhexyl) thien-2-yl)-benzo[1,2-*b*:4,5-*b*′]dithiophene **(1)**,[16] 2,6-bis(4-octylthiophen-2-yl)benzo[1,2-*d*; 5,4-*d*′]bisoxazole **(2)**,[7(f)] 2,6-bis(4-octylthiophen-2-yl)benzo[1,2-*d*; 4,5-*d*′]bisoxazole **(3)**,[7(f)] and 2,6-bis(4-octylthiophen-2-yl)benzo[1,2-*d*; 4,5-*d*′]bisthiazole **(4)**[7(f)] were synthesized according to literature procedures. All other compounds were purchased from commercial sources and used without further purification. Nuclear magnetic resonance (NMR) spectra were carried out in $CDCl_3$ and recorded on Varian VXR (300 MHz), Varian MR (400 MHz), or a Bruker Avance-III (600 MHz). ^{1}H NMR spectra were internally referenced to the residual protonated solvent peak. In all spectra, chemical shifts are given in ppm (δ) relative to the solvent. Gel permeation chromatography (GPC) measurements were performed on a separation module equipped with two 10-μm AMGPC-gel columns (crosslinked styrene-divinyl benzene copolymer) connected in series (guard, 10,000 Å, 1000 Å) with a UV–vis detector. Analyses were performed at 40 °C temperature using chloroform as the eluent with a flow rate of 1.0 mL min^{-1}. Calibration was based on polystyrene standards. Thermogravimetric analysis (TGA) measurements were performed over an interval of 30–850 °C at a heating rate of 20 °C min^{-1} under ambient atmosphere. Cyclic voltammetry was performed using a e-DAQ e-corder 410 potentiostat with a scanning rate of 100 mV s^{-1}. The polymer solutions (1–2 mg mL^{-1}) were drop-cast onto a platinum electrode. Ag/Ag^+ was used as the reference electrode and a platinum wire as the auxiliary electrode. The reported values are referenced to Fc/Fc^+ (−4.8 eV vs. vacuum). All electrochemistry experiments were performed in deoxygenated CH_3CN under an argon atmosphere using 0.1 M tetrabutylammonium hexafluorophosphate as the electrolyte. Absorption spectra were obtained on a photodiode-array Agilent 8453 UV–visible spectrophotometer using polymer solutions in $CHCl_3$ and thin films. The films were made by spin-coating 25 × 25 × 1-mm glass slides using solutions of polymer (2 mg/mL) in 1:1 $CHCl_3$/*o*-dichlorobenzene mixture at a spin rate of 1200 rpm on a Headway Research PWM32 spin-coater.

General Polymerization Procedure

A mixture of **1** and the respective benzobisazole, 2 mol % tris(dibenzylideneacetone)dipalladium(0), 8 mol % tris(*o*-tolyl)phosphine in 7 mL of deoxygenated toluene was charged in a round-bottom flask equipped with a reflux condenser and an argon inlet. The mixture was allowed to reflux for 18–72 h before it was end-capped by addition of trimethyl(phenyl)tin followed by iodobenzene. The polymer was precipitated into 100 mL of cold methanol and filtered through an extraction thimble. The polymer was successively washed with methanol, hexanes, and extracted with chloroform. The chloroform fraction was allowed to stir overnight at 50 °C with functionalized silica gel (SiliaMetS® Cysteine). The chloroform fraction was then filtered through a bed of Celite and the solvent was removed under reduced pressure. The polymer was further purified with a short silica gel plug using chloroform as the eluent. It was then precipitated in methanol, filtered, and dried under vacuum.

Synthesis of P1

Following the general polymerization procedure using compounds **1** (200 mg, 0.22 mmol) and **2** (156 mg, 0.22 mmol) and a reaction time of 72 h afforded a dark solid (154 mg, 76%). GPC ($CHCl_3$, 40 °C): $M_n = 15.9$ kDa, $Đ = 1.9$.

Synthesis of P2

Following the general polymerization procedure using compounds **1** (200 mg, 0.22 mmol) and **3** (156 mg, 0.22 mmol) and a reaction time of 72 h afforded a dark solid (143 mg, 71%). GPC ($CHCl_3$, 40 °C): $M_n = 10.9$ kDa, $Đ = 2.1$.

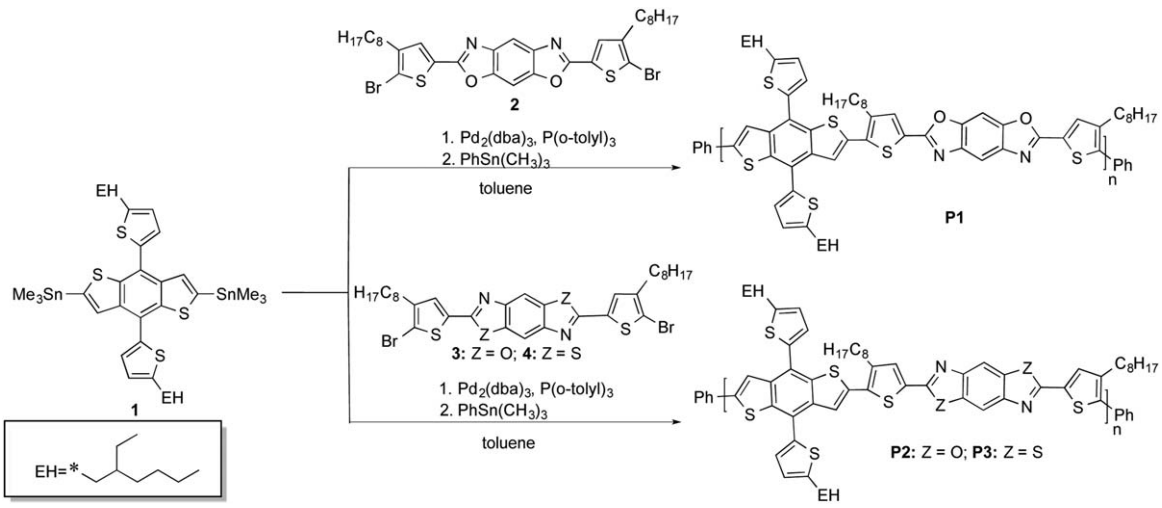

SCHEME 1 Synthesis of benzodithiophene–thiophene–benzobisazole copolymers.

Synthesis of P3

Following the general polymerization procedure using compounds **1** (80 mg, 0.09 mmol) and **4** (65 mg, 0.09 mmol) and a reaction time of 18 hours afforded a dark solid (70 mg, 60%). GPC ($CHCl_3$, 40 °C): $M_n = 5.3$ kDa, $Đ = 1.5$.

Device Fabrication and Characterization

All devices were produced via a solution-based, spin-casting fabrication process. All polymers were mixed with $PC_{71}BM$ (SES Research) (mixed 1:2.5 (*w/w*) with a total solution concentration of 21 mg mL^{-1}) then dissolved in *o*-dichlorobenzene and stirred at 90 °C for 48 h. Indium tin oxide (ITO) (20–25.2 Ω)-coated glass slides (Delta Technologies) were cleaned by consecutive 10-min sonications in (i) Mucasol™ detergent (dissolved in deionized water), 2×, (ii) deionized water, (iii) acetone, and then (iv) isopropanol. The slides were then dried in an oven for at least 3 h and cleaned with air plasma (Harrick Scientific plasma cleaner) for 10 min. Filtered (0.45 μm) [poly(3,4-ethylene dioxythiophene): poly(styrene sulfonate)] (PEDOT:PSS) (Clevios P™) was spin-coated onto the prepared substrates (2000 rpm/60 s) after first being stirred for 10 min at room temperature. The PEDOT:PSS films were annealed at 150 °C for 30-min air and transferred to an nitrogen-filled glovebox after cooling. After 48 h of mixing, the polymer:$PC_{71}BM$ solutions were filtered (0.45-μm pore, GS-Tek) and simultaneously dropped onto the PEDOT:PSS-coated substrates and spin-cast at 1000 rpm for 60 s. The films were dried under vacuum overnight. Ca (20 nm) and Al (100 nm) were successively thermally evaporated through a shadow mask (area = 0.06 cm^{-2}) under vacuum of 10^{-6} mbar to complete the devices. *J–V* data were generated by illuminating the devices using an ETH quartzline lamp at 1 sun (calibrated using a crystalline silicon photodiode with a KG-5 filter). The hole mobility was extracted from the space-charge-limited current (SCLC) measurement using keithley 2400 source/meter in the dark under ambient condition.

Atomic Force Microscopy

All measurements were performed on films cast as described above; electrodes were not attached to these samples. A Veeco Digital Instruments atomic force microscope (AFM) was used to perform the analysis. The tapping-mode AFM was carried out using TESPA tip with scan rate of 0.5 μm s^{-1} and scan size of 3 × 3 μm^2.

RESULTS AND DISCUSSION

Synthesis and Physical Characterization

The synthesis of the polymers is shown in Scheme 1. The required monomers 4,8-bis(5-(2-ethylhexyl) thien-2-yl)-benzo[1,2-*b*:4,5-*b*′]dithiophene **1**,[16] 2,6-bis(4-octylthiophen-2-yl)-benzo[1,2-*d*; 5,4-*d*′]bisoxazole **2**,[7(f)] 2,6-bis(4-octylthiophen-2-yl)-benzo[1,2-*d*; 4,5-*d*′]bisoxazole **3**,[7(f)] and 2,6-bis(4-octylthiophen-2-yl)-benzo[1,2-*d*; 4,5-*d*′]bisthiazole **4**[7(f)] were synthesized according to the literature procedure. The use of the thiophene–benzobisazole–thiophene triad prevents ring opening side reactions at the 2- and 6-positions of the benzobisazole ring during the cross-coupling reaction.[17] The Stille cross-coupling polymerization of monomer **1** with **2**, **3**, or **4** with afforded polymers **P1**, **P2**, and **P3**, respectively, in yields ranging from 60 to 76%. All polymers had limited solubility in common organic solvents, such as THF, and chloroform at room temperature, preventing characterization via NMR spectroscopy. However, characterization via GPC was possible and the results are shown in Table 1 and Supporting Information Figures S5–S7. The reported molecular weight of **P3** appears to be half that of **P1** and **P2** due to the reduced solubility of the sulphur-containing polymer. We also believe that the limited solubility of **P3** has impeded its analysis as only the fraction soluble in chloroform at room temperature was evaluated. Nonetheless, all of the polymers showed excellent film-forming abilities. TGA revealed that all polymers were thermally stable with 5% weight loss onsets occurring above 240 °C under air (Supporting Information Fig. S8). The results are summarized in Table 1.

TABLE 1 Physical Characterization of **P1–P3**

Polymer	Yield[a] (%)	M_n[b] (kDa)	$Đ$[b]	DP$_n$	T_d (°C)[c]
P1	76	15.9	1.9	17	387
P2	71	10.9	2.1	12	246
P3	60	5.3	1.5	4	250

[a] Isolated yield.
[b] Determined by GPC in $CHCl_3$ using polystyrene standards.
[c] 5% weight loss temperature by TGA in air.

Optical and Electrochemical Properties

The normalized absorbance spectra of the polymer solutions in chloroform and in the solid state are shown in Figures 1 and 2, respectively, and the data are summarized in Table 2. In solution, the UV–visible spectrum for **P2** has a single, featureless absorbance band, whereas vibronic coupling is seen in the spectra of **P1** and **P3**. The absorption maximum for **P2** is hypsochromically shifted 26 nm relative to the absorbance maximum for its isomer, **P1**, whereas the absorption maximum of **P3** is red-shifted 87 nm relative to the isoelectronic **P2**. All of the spectra are fairly broad and lack a second low-energy absorption seen when intermolecular charge transfer between the electron-donating and electron-accepting units is occurring.[3(c)] As thin films, the absorbance maximum for all of the polymers are bathochromically shifted indicating increased backbone planarization and π-stacking in the solid state.[18] Interestingly, the absorbance maxima of **P1** and **P2** in thin film are significantly red-shifted relative to their solution spectra, while the absorbance maxima of **P3** is only slightly red-shifted relative to its solution spectra. The difference is likely a result of the lower molecular weight of **P3**. Despite the lower molecular weight of the polymer, **P3** exhibited the most red-shifted absorbance maximum of the series. Overall, the absorption maxima for these polymers is also red-shifted relative to the analogous quarter thiophene benzobisazoles, which had absorption maxima of 460, 475, and 462 nm for the *cis*-BBO, *trans*-BBO, and *trans*-BBZT polymers, respectively, and similar molecular weights.[10(c)] Although the optical band gaps for both series of polymers were similar, the red-shifted absorption in this series of polymers is beneficial in improving the photovoltaic properties of the polymers.

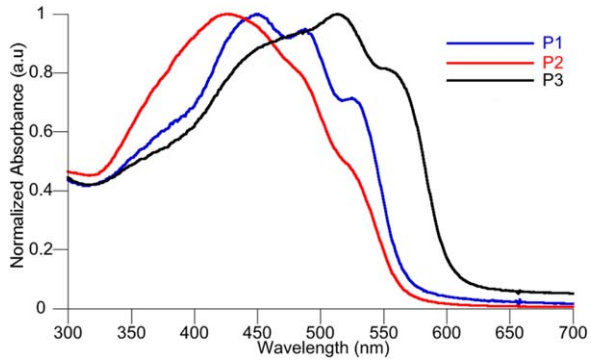

FIGURE 1 UV–vis absorption spectra of **P1–P3** in dilute chloroform solutions. [Color figure can be viewed in the online issue, which is available at wileyonlinelibrary.com.]

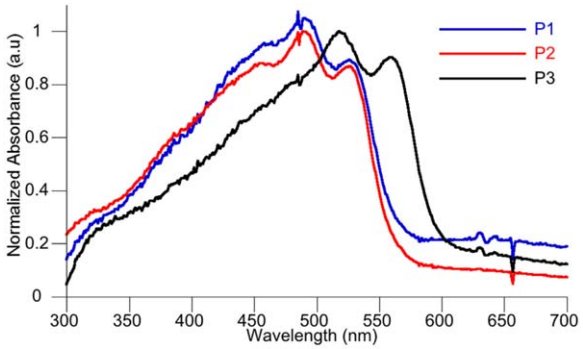

FIGURE 2 UV–vis absorption spectra of **P1–P3** as thin films spun from polymer solutions in *o*DCB (2 mg/mL). [Color figure can be viewed in the online issue, which is available at wileyonlinelibrary.com.]

The electrochemical properties of the polymers were evaluated by cyclic voltammetry. All three polymers exhibit measureable and reproducible oxidation and reduction processes (Supporting Information Fig. S9). The HOMO and LUMO levels were estimated from the onset of oxidation and reduction using the absolute energy level of ferrocene/ferrocenium (Fc/Fc^+) as -4.8 eV under vacuum and are summarized in Table 2.[19] The HOMO levels ranged from -5.2 to -5.3 eV, all of which are deep enough to guarantee good air stability.[20] The LUMO levels ranged from -3.1 to -3.5 eV, with the *trans*-BBZT being the lowest. As a result, **P3** had the smallest electrochemical band gap of the series. The electrochemical band gaps for **P1** and **P2** are both similar to their optical band gaps, whereas the electrochemical band gap of **P3** is significantly smaller than its optical band gap. We note that the current of the cyclic voltammogram of **P3** is also smaller than that of the other polymers which could be a result of difference in the morphology of the polymer film on the electrodes surface among other issues.[19] These data demonstrates that changing the position of the oxygen atoms from the cis- configuration to the trans- configuration has a negligible impact on the HOMO level and a negligible impact on the LUMO level. However, replacing the oxygen atoms of *trans*-BBO with sulfur had a negligible impact on the HOMO level, while reducing the LUMO level by ~0.3 eV. As a result, the benzobisthiazole polymer has the smallest electrochemical band-gap.

Previously, we were able to evaluate the energy levels using both CV and ultraviolet photoelectron spectroscopy (UPS) and saw good correlation between both measurements. UPS provides a more accurate values for the HOMO level than CV.[21] Based on the UPS measurements, switching the orientation of oxygen within benzobisoxzole from *cis* to *trans* lowered the HOMO level by 0.1 eV, and substituting the oxygen atoms in *trans*-BBO with sulfur atoms had no effect on the HOMO level. Conversely, switching the orientation within benzobisoxzole from *cis* to *trans* lowered the LUMO level by

TABLE 2 Electronic and Optical Properties of Benzobisazole–Thiophene–Dithienosilole Terpolymers

	Solution	Film							
Polymer	λ_{max}^{soln} (nm)	λ_{max}^{film} (nm)	λ_{onset} (nm)	E_g^{opt} (eV)[a]	E_g^{EC} (eV)[b]	E_{onset}^{ox}	E_{onset}^{red}	HOMO (eV)[c]	LUMO (eV)[d]
P1	451	490	565	2.2	2.1	0.42	−1.70	−5.2	−3.1
P2	425	487	575	2.2	2.1	0.46	−1.59	−5.3	−3.2
P3	513	518	600	2.1	1.7	0.35	−1.35	−5.2	−3.5

[a] Estimated from the optical absorption edge.
[b] Estimated from HOMO to LUMO.
[c] HOMO = $-4.8-(E_{onset}^{ox})$ (eV).
[d] LUMO = $-4.8-(E_{onset}^{red})$ (eV). Electrochemical properties were measured using a three-electrode cell (electrolyte: 0.1 mol/L $TBAPF_6$ in acetonitrile) with an Ag/Ag^+ reference electrode, a platinum auxiliary electrode, and a platinum-button working electrode. Reported values are referenced to Fc/Fc^+. Polymer films were drop cast from an *ortho*-dichlorobenzene (*o*DCB) solution of the polymers on to the working electrode. All cyclic voltammetry experiments were recorded at a scan rate of 50 mV/s.

0.1 eV, whereas replacing the oxygen atoms in *trans*-BBO with sulfur atoms raised the LUMO level by 0.1 eV. The LUMO levels of **P1** and **P2** are both 0.2 eV lower than those reported previously for the analogous quarterthiophene benzobisoxazole polymers (−2.9 eV) and the HOMO levels are both 0.1 eV higher (−5.3 and −5.4 eV).[10(c)] However, **P3** has a significantly lower LUMO level than its quarterthiophene analog (−3.1 eV) and the HOMO level is 0.2 eV higher (−5.4 eV).[10(c)]

Evaluation of Charge Carrier Mobility and Photovoltaic Properties

The performance of all three polymers in OPVs were evaluated using $PC_{71}BM$ as the electron acceptor with a device configuration of ITO/PEDOT:PSS/polymer:$PC_{71}BM$/Ca/Al. Photovoltaic devices with this configuration were fabricated using different polymer:$PC_{71}BM$ weight ratios and are summarized in Supporting Information Table S1. The active layer was deposited from 21 mg/mL *o*-DCB solutions, using processing conditions selected to give a thickness of approximately 100 nm. In all cases, the best performance was obtained using a 1:2.5 weight ratio of polymer to $PC_{71}BM$. The current density–voltage (*J–V*) curves of **P1**:$PC_{71}BM$, **P2**:$PC_{71}BM$, and **P3**:$PC_{71}BM$ photovoltaic devices at this weight ratio under AM 1.5 G illumination (100 mW cm^{-2}) are shown in Figure 3. These devices were evaluated with and without the solvent additive, 1,8-diiodooctane (DIO). The resulting photovoltaic performances including short circuit current density (J_{SC}), open circuit voltage (V_{OC}), fill factor (FF), and PCE are shown in Table 3. The external quantum efficiencies (EQEs) of the solar cell devices were also examined. The EQE curves for the solar cells fabricated under the same conditions used for the *J–V* measurements are shown in Supporting Information Figure S10. The trend in the EQE values is consistent with the observed performance for the cells. Overall, the devices based on **P2** gave the highest PCE at 2.78% without the use of solvent additives. The devices made from **P1** and **P3** had lower efficiencies with values of 1.75 and 1.62%, respectively. Although all of the polymers had similar V_{OC} and FF, **P2** had the highest photocurrent, and as a result, the highest PCE. This is almost a threefold improvement over the previously reported poly(quarterthiophene benzobisoxazole).[10(c)] Interestingly, the **P1**- and

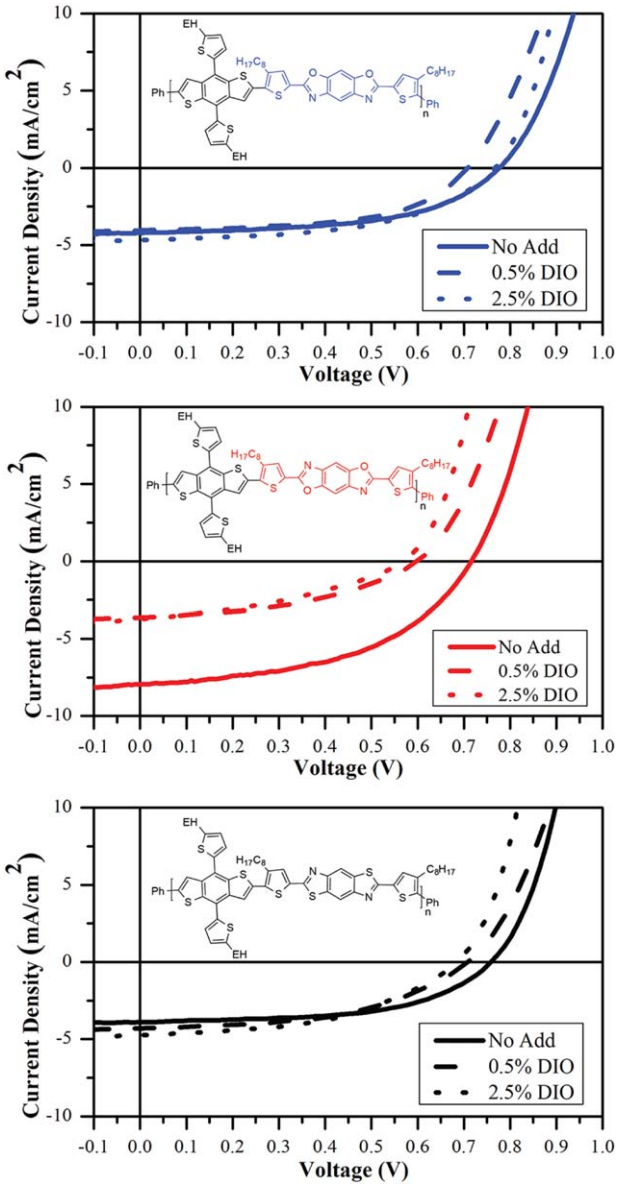

FIGURE 3 Current density–voltage *(J–V)* curves of polymer:$PC_{71}BM$, photovoltaic devices under AM 1.5 G illumination (100 mW cm^{-2}). [Color figure can be viewed in the online issue, which is available at wileyonlinelibrary.com.]

TABLE 3 Photovoltaic Device Performance of **P1–P3** with $PC_{71}BM$

Polymer	Additive (% DIO)	J_{SC} (mA/cm^2)	V_{OC} (V)	FF	PCE (%)	Max PCE (%)	R_{SH} (Ω cm^2)
P1	None	4.05 ± 0.15	0.79 ± 0.01	0.53 ± 0.0	1.71 ± 0.03	1.75	457 ± 259
P1	0.5%	3.99 ± 0.05	0.70 ± 0.00	0.56 ± 0.0	1.57 ± 0.04	1.61	1,656 ± 127
P1	2.5%	4.52 ± 0.14	0.76 ± 0.02	0.53 ± 0.1	1.78 ± 0.07	1.85	982 ± 134
P2	None	7.81 ± 0.18	0.72 ± 0.01	0.49 ± 0.0	2.74 ± 0.05	2.78	818 ± 209
P2	0.5%	3.31 ± 0.21	0.59 ± 0.01	0.43 ± 0.0	0.87 ± 0.07	0.94	792 ± 34
P2	2.5%	3.74 ± 0.00	0.55 ± 0.02	0.37 ± 0.0	0.76 ± 0.04	0.79	708 ± 37
P3	None	3.79 ± 0.08	0.76 ± 0.01	0.55 ± 0.0	1.58 ± 0.04	1.62	944 ± 455
P3	0.5%	4.26 ± 0.08	0.69 ± 0.02	0.51 ± 0.2	1.50 ± 0.00	1.50	970 ± 40
P3	2.5%	4.60 ± 0.04	0.68 ± 0.01	0.48 ± 0.0	1.53 ± 0.03	1.54	835 ± 146

Photovoltaic devices with a configuration of ITO/PEDOT:PSS/Polymer:$PC_{71}BM$/Ca/Al were fabricated at a 1:2.5 weight ratio of polymer to $PC_{71}BM$ and a total solution concentration of 21 mg mL^{-1}. DIO was used as the additive (% v/v). Averages are based on 6 devices.

P3-based devices had similar performances with respective values of 1.85 and 1.62%, despite the significantly lower molecular weight of **P3**, which can negatively affect film formation and charge carrier mobility.[22] The OPV performance of **P3** is comparable to that reported by Jenekhe et al. for a related benzobisthiazole polymer, poly[(4,8-bis(2-hexyldecyl) oxy)benzo[1,2-*b*:4,5-*b*′]dithiophene)−2,6-diyl-alt-(2,5-bis(3-dodecylthiophen-2-yl)benzo[1,2-*d*;4,5-*d*′]bisthiazole)] (PBTHDDT), which had a PCE of 1.76%, that improved to 2.96% with the use of additives.[10(a)] We also evaluated the use of DIO as a solvent additive,[23] but only observed a nominal improvement in the PCE for **P1**, and a decrease in the performance of **P2** and **P3**. However, PBTHDDT differs from our polymer in the placement and nature of the substituents on both the thiophenes and benzodithiophene. This suggests that additional optimization of our system could yield an even higher PCE.

The mobilities were calculated according to eq 1: The hole mobility of the polymers was examined using the SCLC method with a hole only device structure of ITO/PEDOT:PSS/Polymer:$PC_{71}BM$/Al.[24] The mobilities were calculated according to the eq 1:

$$\mathbf{J}_{\mathrm{SCLC}} = \frac{9\varepsilon_0\varepsilon_r\mu_h V^2}{8L^3} \quad (1)$$

where $\varepsilon_0\varepsilon_r$ is the permittivity of the polymer, μ_h is the carrier mobility, and L is the device thickness.[25] The hole mobilities were determined to be 2.19×10^{-5}, 2.18×10^{-5}, and 6.58×10^{-5} cm^{2}V^{-1}s^{-1} for **P1**, **P2**, and **P3**, respectively. These values are all of the same order of magnitude which indicates that the difference in the PCE of the polymers is not a function of their charge carrier mobility.

The surface roughness and phase distribution of the three polymer systems were studied by AFM (Fig. 4). The AFM height images revealed that both the **P1**:$PC_{71}BM$ and **P2**:$PC_{71}BM$ blend films have large domain sizes, manifesting root-mean square (RMS) surface roughness values of 2.94 and 1.20 nm, respectively. Whereas, the **P3**:$PC_{71}BM$ blend film has smaller domains (RMS = 0.78 nm). The AFM phase images of **P2**:$PC_{71}BM$ film displays a refined morphology that improves the exciton dissociation efficiency and, thus, the PCE. Conversely, films of the **P1**:$PC_{71}BM$ and **P3**:$PC_{71}BM$ blend show poor intermixing between polymer and fullerene, reducing overall efficiency. Our previous X-ray diffraction studies on poly(quarter thiophene benzobisazoles) indicate that the structural differences in the materials do not significantly impact the packing of the polymer chains.[10(c)] Therefore, the differences in the morphology of these polymers are likely a result of differences in solubility. Supporting Information Figures S11–S13 show the AFM surface roughness and phase images of the three polymer systems were captured at 0.5 and 2.5% DIO additives. The RMS values of the films topography (shown in Supporting Information Fig. S14) indicate that the DIO additive increases the film roughness and the polymer/fullerene phase separation as depicted in the phase images of Supporting Information Figures S11–S13. This is true for **P1**- and **P2**-based thin films. Whereas, **P3**:PC71BM thin film that showed slight increase in the domain sizes of polymer and fullerene. The observed phase separation with DIO additive hampers the charge dissociation efficiency and, thus, the photovoltaic characteristics (Table 3). It is worth mentioning that the **P2**:PCBM thin films show an RMS increase from 0.91 nm for the control (no additive) to 1.75 and 2.54 nm for the 0.5 and 2.5% of DIO additives, respectively (Table 4). This strongly affects the P2:PC71BM intermixing, revealing average (max) PCEs of 2.54 (2.78), 0.87 (0.94) and 0.74 (0.79)% for the control, 0.5 and 2.5% DIO additives, respectively (Supporting Information Fig. S14).

CONCLUSIONS

Three terpolymers composed of thiophene, benzodithiophene, and benzobisazoles were prepared in an effort to develop efficient materials for use in photovoltaic cells. The benzobisoxazole polymers had good solubility in various organic solvents, whereas the *trans*-benzobisthiazole polymer had limited solubility preventing the synthesis of high molecular weight polymer. All of the polymers had similar HOMO

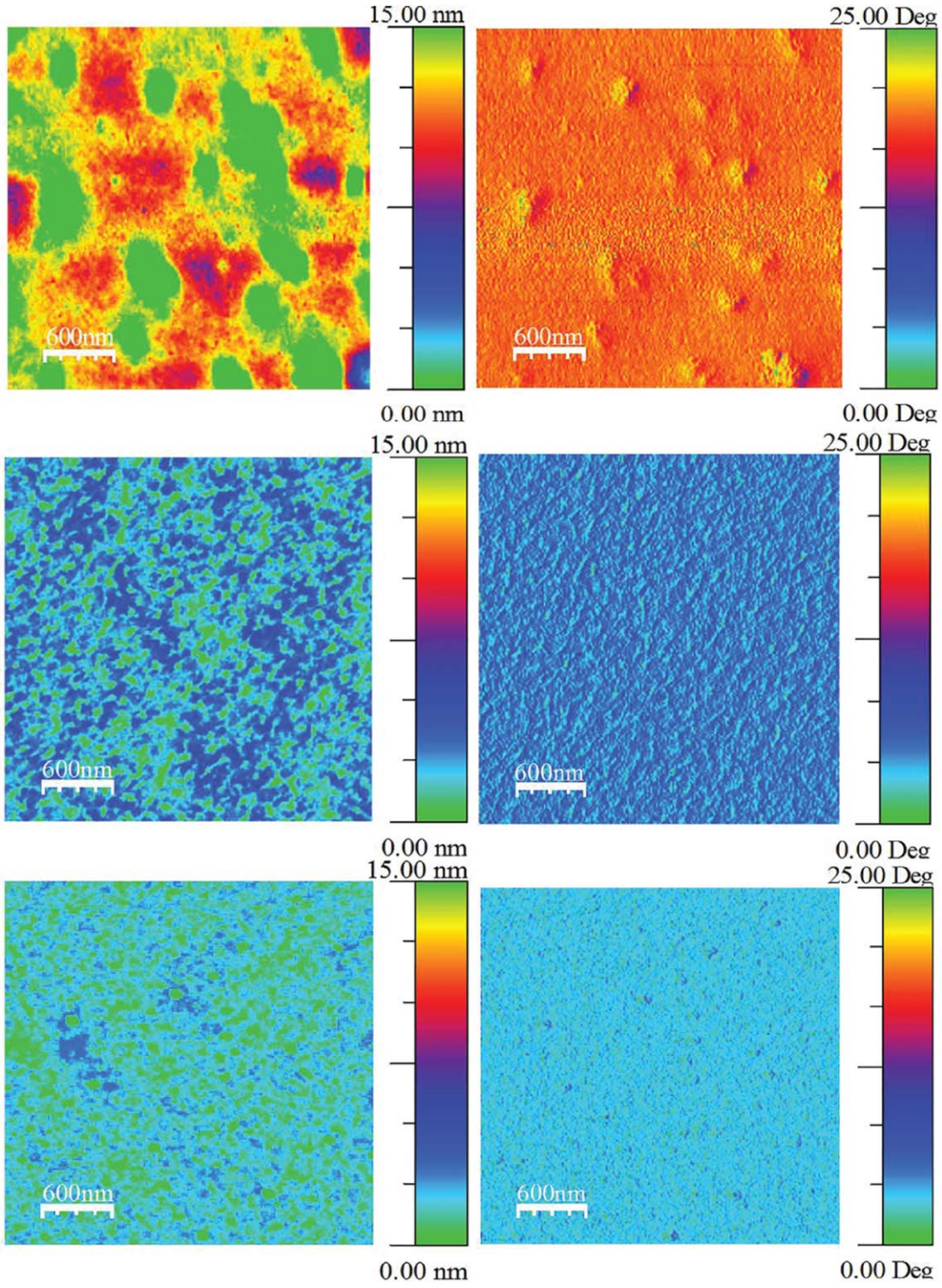

FIGURE 4 AFM height (left) and phase (right) images at 3 × 3 μm^2 of devices with polymer:$PC_{71}BM$ blends at a 1:2.5 weight ratio. From top to bottom: P1:$PC_{71}BM$, P2:$PC_{71}BM$, and P3:$PC_{71}BM$.

levels, but different LUMO levels and fairly wide band gaps. The *trans*-benzobisthiazole polymer, **P3**, exhibited slightly broader and red-shifted absorption spectra relative to the other benzobisazoles in the solid state. Furthermore, this polymer also had the highest hole mobility of all three polymers. However, these properties did not translate into better performance in OPVs as the polymer based on *trans*-benzobisoxazole gave the best performance of the series at 2.78%. The poor performance of the *trans*-benzobisthiazole polymer is likely a result of the negative impact the molecular weight

TABLE 4 Hole Mobility of **P1–P3** Hole-Only Devices, and AFM Data of Polymer: $PC_{71}BM$ Blends

Polymer	μ_h ($cm^2\ V^{-1}\ s^{-1}$)	RMS Roughness (nm)
P1	2.19×10^{-5}	2.94
P2	2.18×10^{-5}	1.20
P3	6.58×10^{-5}	0.78

has on the active layer film morphology. At the same time, the OPV performance of all these polymers is limited due to the wide band gap and relatively high-lying HOMO level. Given the overall ease of synthesis, benzobisazoles are still promising building blocks for the development of OPV materials. However, additional improvements in solubility, processing, and electronic properties are needed. Accordingly, we are actively pursuing the synthesis of new derivatives to address the wide band gap and processibility of these polymers.

ACKNOWLEDGMENTS

The authors thank the National Science Foundation (DMR-0846607) for partial support of this work. They also thank the National Science Foundation Materials Research Facilities Network (DMR-0820506) and Polymer-Based Materials for Harvesting Solar Energy, an Energy Frontier Research Center funded by the U.S. Department of Energy, Office of Science, Office of Basic Energy Sciences under Award Number DE-SC0001087 for support of the device fabrication. The Iowa State University (ISU) Institute for Physical Research and Technology provided MDE with a Catron Fellowship. Some of the OPV work was performed at the ISU Microelectronics Research Center. They also thank Michael Zenner for thermal analysis. M. Elshobaki thanks the financial support from the Egyptian government (scholarship # GM915).

REFERENCES AND NOTES

1 G. Yu, J. Gao, J. C. Hummelen, F. Wudl, A. Heeger, *J. Sci.* **1995**, *270*, 1789–1791.

2 H. Zhou, L. Yang, W. You, *Macromolecules* **2012**, *45*, 607–632.

3 (a) H. A. M. van Mullekom, J. A. J. M. Vekemans, E. E. Havinga, E. W. Meijer, Mater. Sci. Eng. R **2001**, *32*, 1–40; (b) E. E. Havinga, W. ten Hoeve, H. Wynberg, *Polym. Bull.* **1992**, *29*, 119–126; (c) P. M. Beaujuge, C. M. Amb, J. R. Reynolds, *Acc. Chem. Res.* **2010**, *43*, 1396–1407.

4 (a) C. M. Amb, S. Chen, K. R. Graham, J. Subbiah, C. E. Small, F. So, J. R. Reynolds, J. Am. Chem. Soc. **2011**, *133*, 10062–10065; (b) Facchetti, A. *Chem. Mater.* **2011**, *23*, 733–758.

5 (a) J. F. Wolfe, F. E. Arnold, Macromolecules **1981**, *14*, 909–915; (b) J. F. Wolfe, B. H. Loo, F. E. Arnold, Macromolecules **1981**, *14*, 915–920; (c) E. W. Choe, S. N. Kim, *Macromolecules* **1981**, *14*, 920–924.

6 S. A. Jenekhe, J. A. Osaheni, J. S. Meth, H. Vanherzeele, *Chem. Mater.* **1992**, *4*, 683–687.

7 (a) J. A. Osaheni, S. A. Jenekhe, Macromolecules **1993**, *26*, 4726–4728; (b) J. Intemann, J. Mike, M. Cai, S. Bose, T. Xiao, T. Mauldin, R. Roggers, J. Shinar, R. Shinar, M. Jeffries-EL, *Macromolecules* **2011**, *44*, 248–255; (c) J. J. Intemann, J. F. Mike, M. Cai, C. A. Barnes, T. Xiao, R. A. Roggers, J. Shinar, R. Shinar, M. Jeffries-EL, *J. Polym. Sci. Part A: Polym. Chem.* **2013**, *51*, 916–923; (d) J. J. Intemann, E. S. Hellerich, B. C. Tlach, M. D. Ewan, C. A. Barnes, A. Bhuwalka, M. Cai, J. Shinar, R. Shinar, M. Jeffries-EL, *Macromolecules* **2012**, *45*, 6888–6897; (e) E. S. Hellerich, J. J. Intemann, M. Cai, R. Liu, M. D. Ewan, B. C. Tlach, M. Jeffries-EL, R. Shinar, J. Shinar, *J. Mater. Chem. C* **2013**, *1*, 5191–5199; (f) J. F. Mike, J. J. Intemann, M. Cai, T. Xiao, R. Shinar, J. Shinar, M. Jeffries-EL, *Polym. Chem.* **2011**, *2*, 2299–2305.

8 M. M. Alam, S. A. Jenekhe, *Chem. Mater.* **2002**, *14*, 4775–4780.

9 (a) I. Osaka, K. Takimiya, R. D. McCullough, Adv. Mater. **2010**, *22*, 4993–4997; (b) E. Ahmed, A. L. Briseno, Y. Xia, S. A. Jenekhe, *J. Am. Chem. Soc.* **2008**, *130*, 1118–1119; (c) E. Ahmed, F. S. Kim, H. Xin, S. A. Jenekhe, *Macromolecules* **2009**, *42*, 8615–8618; (d) H. Pang, F. Vilela, P. J. Skabara, J. J. W. McDouall, D. J. Crouch, T. D. Anthopoulos, D. D. C. Bradley, D. M. de Leeuw, P. N. Horton, M. B. Hursthouse, *Adv. Mater.* **2007**, *19*, 4438–4442.

10 (a) E. Ahmed, S. Subramaniyan, F. S. Kim, H. Xin, S. A. Jenekhe, Macromolecules **2011**, *44*, 7207–7219; (b) A. V. Patil, H. Park, E. W. Lee, S.-H. Lee, *Synth. Met.* **2010**, *160*, 2128–2134; (c) A. Bhuwalka, J. F. Mike, M. He, J. J. Intemann, T. Nelson, M. D. Ewan, R. A. Roggers, Z. Lin, M. Jeffries-EL, *Macromolecules* **2011**, *44*, 9611–9617; (d) S. Subramaniyan, F. S. Kim, G. Ren, H. Li, S. A. Jenekhe, *Macromolecules* **2012**, *45*, 9029–9037; (e) A. Saeki, M. Tsuji, S. Yoshikawa, A. Gopal, S. Seki, *J. Mater. Chem. A* **2014**, *2*, 6075–6080; (f) M. Tsuji, A. Saeki, Y. Koizumi, N. Matsuyama, C. Vijayakumar, S. Seki, *Adv. Funct. Mater.* **2014**, *24*, 28–36.

11 M. Inbasekaran, R. Strom, *OPPI Briefs* **1994**, *23*, 447–450.

12 (a) J. G. Laquindanum, H. E. Katz, A. J. Lovinger, A. Dodabalapur, Adv. Mater. **1997**, *9*, 36–39; (b) J. Hou, M.-H. Park, S. Zhang, Y. Yao, L.-M. Chen, J.-H. Li, Y. Yang, *Macromolecules* **2008**, *41*, 6012–6018; (c) P. Sista, M. C. Biewer, M. C. Stefan, *Macromol. Rapid Commun.* **2012**, *33*, 9–20; (d) Y. Liang, Z. Xu, J. Xia, S.-T. Tsai, Y. Wu, G. Li, C. Ray, L. Yu, *Adv. Mater.* **2010**, *22*, E135–E138; (e) A. Najari, S. Beaupré, P. Berrouard, Y. Zou, J.-R. Pouliot, C. Lepage-Pérusse, M. Leclerc, *Adv. Funct. Mater.* **2011**, *21*, 718–728.

13 (a) K. Li, Z. Li, K. Feng, X. Xu, L. Wang, Q. Peng, J. Am. Chem. Soc. **2013**, *135*, 13549–13557; (b) L. Dou, J. You, J. Yang, C.-C. Chen, Y. He, S. Murase, T. Moriarty, K. Emery, G. Li, Y. Yang, *Nat. Photon.* **2012**, *6*, 180–185; (c) Y. Liang, D. Feng, Y. Wu, S.-T. Tsai, G. Li, C. Ray, L. Yu, *J. Am. Chem. Soc.* **2009**, *131*, 7792–7799; (d) H.-C. Chen, Y.-H. Chen, C.-C. Liu, Y.-C. Chien, S.-W. Chou, P.-T. Chou, *Chem. Mater.* **2012**, *24*, 4766–4772; (e) Z. He, C. Zhong, S. Su, M. Xu, H. Wu, Y. Cao, *Nat. Photon.* **2012**, *6*, 591–595; (f) S. Zhang, L. Ye, W. Zhao, D. Liu, H. Yao, J. Hou, *Macromolecules* **2014**, *47*, 4653–4659.

14 (a) L. Huo, J. Hou, S. Zhang, H.-Y. Chen, Y. Yang, Angew. Chem. Int. Ed. **2010**, *49*, 1500–1503; (b) L. Ye, S. Zhang, L. Huo, M. Zhang, J. Hou, *Acc. Chem. Res.* **2014**, *47*, 1595–1603.

15 A. Bhuwalka, M. D. Ewan, J. F. Mike, M. Elshobaki, B. Kobilka, S. Chaudhary, M. Jeffries-EL, *J. Polym. Sci. Part A: Polym. Chem.* **2015**, *53*, 1533–1540.

16 J. Yuan, Z. Zhai, H. Dong, J. Li, Z. Jiang, Y. Li, W. Ma, *Adv. Funct. Mater.* **2013**, *23*, 885–892.

17 R. S. Sanchez, F. A. Zhuravlev, *J. Am. Chem. Soc.* **2007**, *129*, 5824–5825.

18 H. Kokubo, T. Sato, T. Yamamoto, *Macromolecules* **2006**, *39*, 3959–3963.

19 C. M. Cardona, W. Li, A. E. Kaifer, D. Stockdale, G. C. Bazan, *Adv. Mater*. **2011**, *23*, 2367–2371.

20 B. C. Thompson, Y. G. Kim, J. R. Reynolds, *Macromolecules* **2005**, *38*, 5359–5362.

21 W. R. Salaneck, *J. Electron Spectrosc. Relat. Phenom*. **2009**, *174*, 3–9.

22 (a) R. J. Kline, M. D. McGehee, E. N. Kadnikova, J. Liu, J. M. J. Frechet, M. F. Toney, Macromolecules **2005**, *38*, 3312–3319; (b) R. Zhang, B. Li, M. C. Iovu, M. Jeffries-EL, G. Sauve, J. Cooper, S. Jia, S. Tristram-Nagle, D. M. Smilgies, D. N. Lambeth, R. D. McCullough, T. Kowalewski, *J. Am. Chem. Soc*. **2006**, *128*, 3480–3481.

23 J. K. Lee, W. L. Ma, C. J. Brabec, J. Yuen, J. S. Moon, J. Y. Kim, K. Lee, G. C. Bazan, A. J. Heeger, *J. Am. Chem. Soc*. **2008**, *130*, 3619–3623.

24 V. D. Mihailetchi, J. Wildeman, P. W. M. Blom, *Phys. Rev. Lett*. **2005**, *94*, 126602.

25 V. Shrotriya, Y. Yao, G. Li, Y. Yang, *Appl. Phys. Lett*. **2006**, *89*, 063505.